

Experimental Analysis of a Gantry Crane of a Shell Structure

Bogusław ŁADECKI, Sławomir BADURA, Filip MATACHOWSKI

AGH University of Science and Technology
Faculty of Mechanical Engineering and Robotics
Al. Mickiewicza 30, 30-059 Kraków, Poland
e-mail: {boglad, sbadura, filip.matachowski}@agh.edu.pl

Gantry cranes of the shell structure are used in Polish steel industry much less than other gantry crane types. Those gantry cranes characterized by increased susceptibility to mechanical vibrations, resulting in greater sensitivity to the formation of fatigue cracks. In this work, measurements of strain gauge bridge deformation of the shells, for which periodically conducted non-destructive testing revealed the presence of numerous fatigue cracks mainly in the area of the under rail beams. Performed periodically repair and reinforcement of the crane did not eliminate the problem of the formation of the subsequent fatigue cracks. The analysis of the dynamic operation of the bridge, in combination with FEM calculations carried out showed stresses exceeding the limit value due to the fatigue phenomena. The results of dynamic analysis can serve as a basis to perform more accurate analysis of the fatigue life of the most intensive areas of the bridge.

Key words: strain gauge measurements, stress state, gantry cranes, FEM, non-destructive testing.

1. INTRODUCTION

Gantry cranes of the shell structure [8, 10] are characterized by very high stiffness and slenderness, their disadvantage is several times lower lifting capacity, compared to the truss structures of comparable sizes, as well as increased susceptibility to mechanical vibrations. Considerations were performed for 350 kN charging gantry crane, operated in one of the Polish steel mills – Fig. 1. For the crane carrier element is a span length of 133 m of the shell structure made of sheet steel reinforced by longitudinally and transversely extending ribs.



FIG. 1. Charging crane of a shell structure.

2. GANTRY CRANE NON-DESTRUCTIVE TESTS

Due to the existence of fatigue cracks after successively executed crane repairs, carried out its comprehensive non-destructive testing [1], in which they are consisted of:

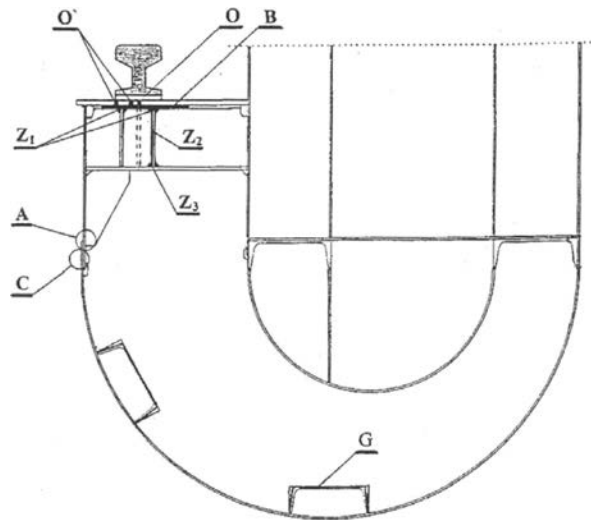
- visual testing the entire outer surface of the crane, in order to determine areas where unacceptable damage to its supporting structure i.e., tears, cracks, permanent deformation or other,
- magnetic particle inspection tests,
- evaluation of the corrosion progress defects using ultrasonic technique,
- analysis of permanent deformation of the span, on the basis of periodic geodetic measurements of the vertical profile shape of the upper belt under rail beams [2].

Made of non-destructive testing [9] revealed a number of areas of cracks, usually on a fatigue nature and other structural damage to the crane. The greatest severity of fatigue cracks were found for under rail beams of the carriage, for which the identified types of damage are illustrated in Figs. 2, 3 and 4.

In addition to occasionally detected cracks “A”, “C” and “G”, for different series of tests were found in total: 42–47% “Z” type cracks, 13–42% “O” cracks type and 8–25% cracks “B” type of the total number of detected cracks. Also in other areas of the crane construction fatigue cracks have occurred, the most serious of which were detected for the shell over the long support leg – Fig. 5.

The increase in crane operational problems, in addition to the above discussed phenomena of fatigue occurring mainly in the area of welded joints of beams under rail also affect maintenance problems in a proper state of carriage railways caused loosening and cracking of numerous bolts, as well as appearing periodically rails cracks.

Exemplary results of the measurements of the crane deflection in mid-span length for two positions of carriage: the short leg axis and the mid-span as



- “A” type – crack of the welded joint in the lower portion of the rib of transverse ribs under rail beam,
- “B” type – crack of the weld connecting the upper shelf ceiling beam with a horizontal shell under rail beam,
- “C” type – vertical crack of the welded joint under rail beam and shell, located between the ribs of the under rail beam,
- “O” type – plate crack under the rail in the direction of the axis of the rail, near the ribs,
- “O’” type – plate crack under the rail parallel to the axis of the rail,
- “Z₁” (“Z₃”) type – weld crack parallel to the axis of the rail, the transverse ribs or rib frames,
- “Z₂” type – vertical joints crack, ribs transverse ribs or frames,
- “G” type – longitudinal butt weld crack (C-section 300).

FIG. 2. Location of the detected cracks of the crane beam.



FIG. 3. Crack of the crane beam detected by the magnetic-powder method type “Z₁” joint 140 mm long.



FIG. 4. Cracks weld of the crane beam stringer type "G" detected by the magnetic-powder method.

a)



b)



FIG. 5. Shell cracks above the long support: a) western side of the bridge – 80 mm and 45 mm long, b) eastern side of the bridge – 80 mm and 45 mm long.

a function of measurement date was shown in Fig. 6. Analysis of measurement results which are presented in Fig. 6 shows that after stabilization of the shape of the beam after the reinforcements after 1993 (years 1993–1996) there is a trend to a slow decline in the value of the deflection to 2003 (results for the years 1998 to 2003) and after the subsequent reinforcement and repair increase in the value of the deflection can be observed registered in the measurements carried out after 2005. Occurring throughout the observation period fluctuations in the value of the deflection are probably connected to: the made cracks repairs in beams, thermal conditions of the measurements, with varying location of the bridge on the length of the track during the course of the next series of measurements as well as other factors such as, for example impact of wind on the structure when conducting geodetic measurements.

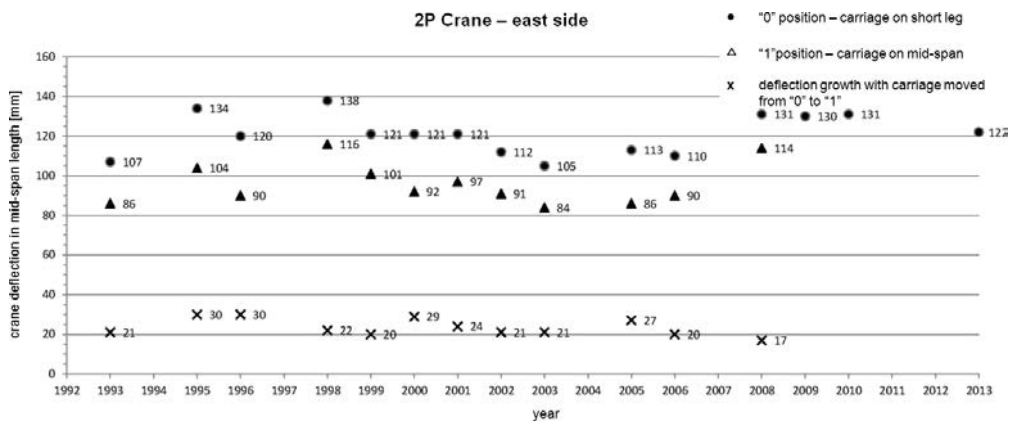


FIG. 6. Results of deflection measurement in the middle of crane's span on east side [1].

Performed periodically repair and reinforcement of the crane did not eliminate the problem of the formation of the subsequent fatigue cracks. In order to clarify the causes of fatigue damage of the bridge was carried out appropriate dynamic analysis of structures based on strain gauge measurements made on a real object deformation, verified by FEM calculations.

3. STRENGHT ANALYSIS

For the discrete model of the crane structure, a total of 17 load cases were examined [4]. FEM analysis [6] showed that for the most unfavorable loads variants of the crane construction, extreme values of shear forces for the span are present in the support area, while the extreme values of bending moments in the support area and in the middle of the span length between supports –

Fig. 7. These areas are consistent with the areas of greatest severity of fatigue cracks in the under rail beams.

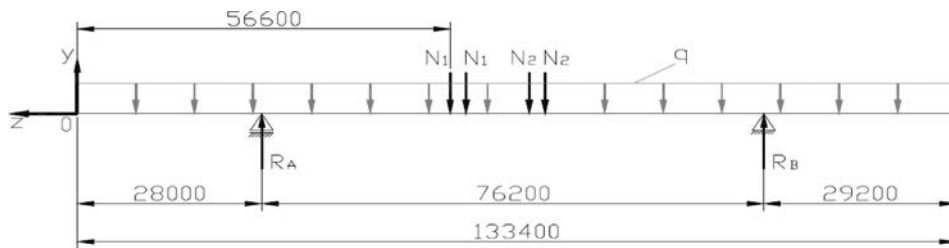


FIG. 7. FEM analysis – load variant 2: beam model with carriage on 56.6 m.

Sample results of reduced stresses obtained in accordance with the hypothesis Huber-Mises, for the span and under rail beam for one of the variants loads are shown in Fig. 8, which also marked the locus of shell cracking shown in Fig. 5, which appeared in place of the notch-induced welding the shell brackets made of L-section, not included in the analysis of the FEM.

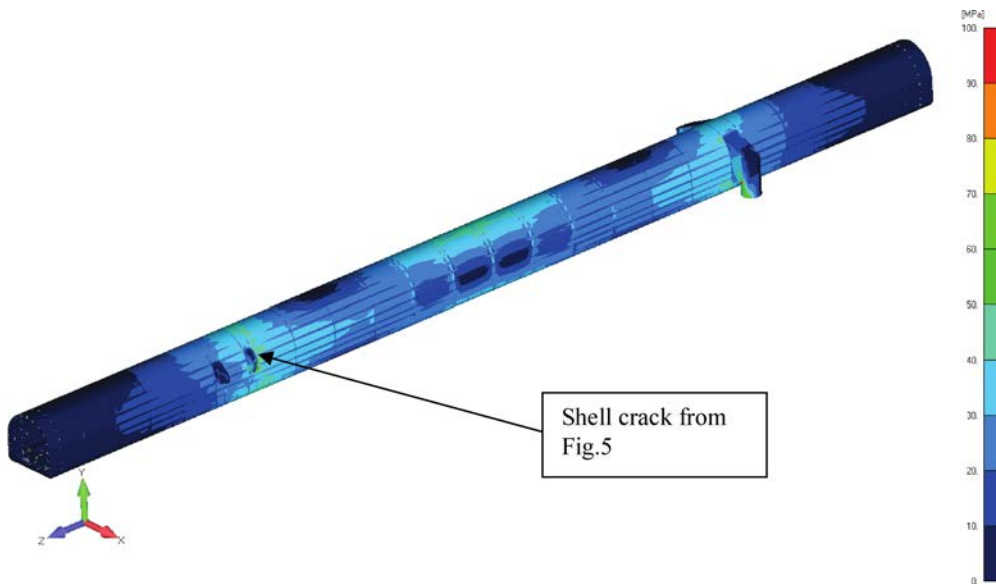


FIG. 8. FEM analysis – distribution of the reduced stresses in the span – load variant 2.

Under rail beam, due to the opening of a fatigue crack was repeatedly repaired during operation, and then reinforced with additional ribs. In order to evaluate the effect of the reinforcements, a comparative analysis of beams without reinforcement – Fig. 9a and beams with reinforcements – Fig. 9b were done. In

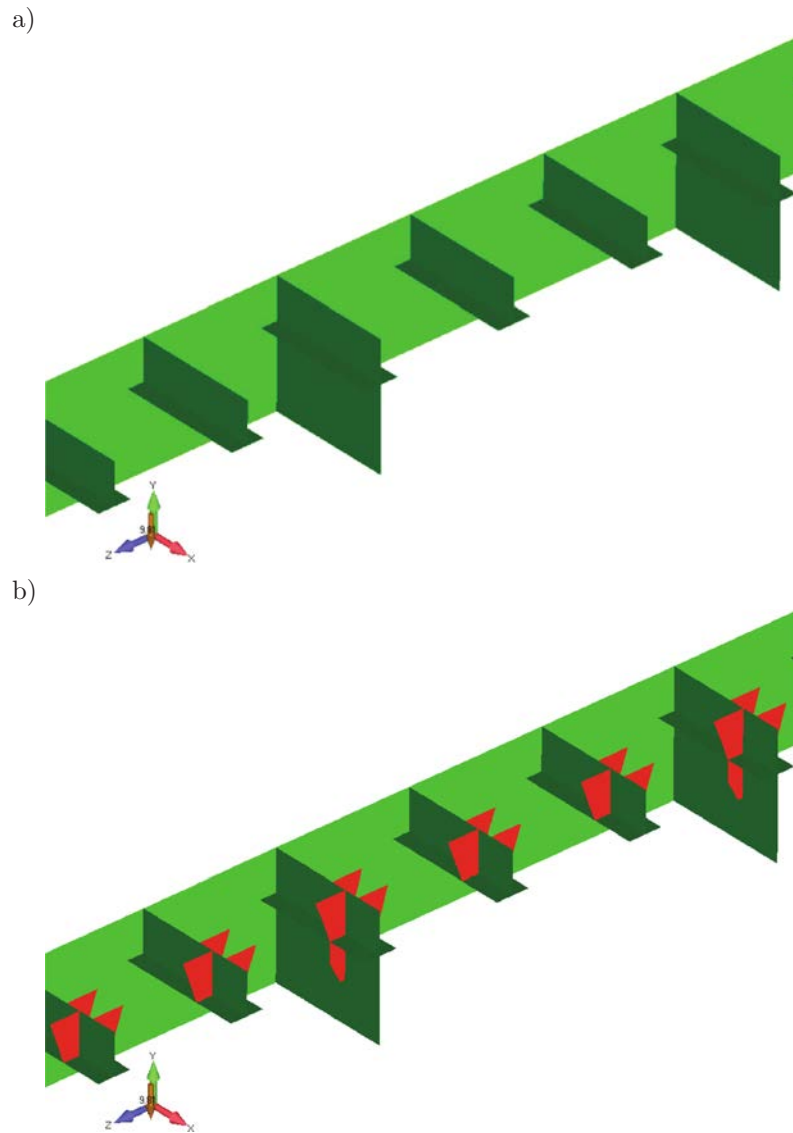
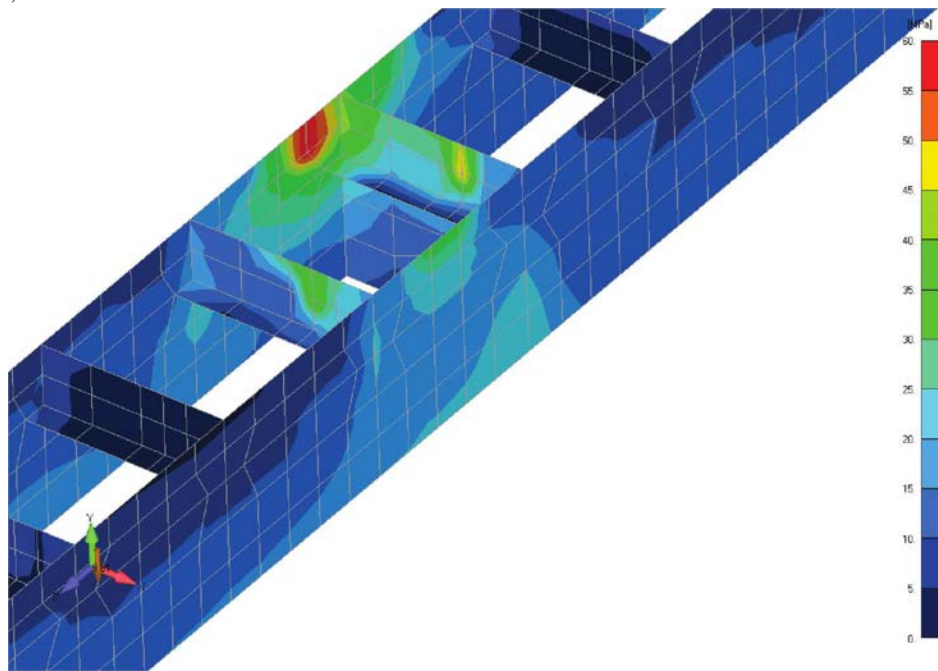


FIG. 9. Inner structure of under rail beam: a) original, b) with additional ribs.

Fig. 10 shows the distribution of reduced Huber-Mises stresses and the values obtained for selected areas of the structure are summarized in Table 1 (values shown in brackets after the application of reinforcing ribs). Extreme reduced stress values for under rail beams without reinforcements, amounting to 65 MPa were obtained for the area of fillet welds cracks type “B” and “Z”. The use of additional reinforcing ribs locally resulted in a reduction of stress cracks in the area “B” and “Z” about to 30%.

a)



b)

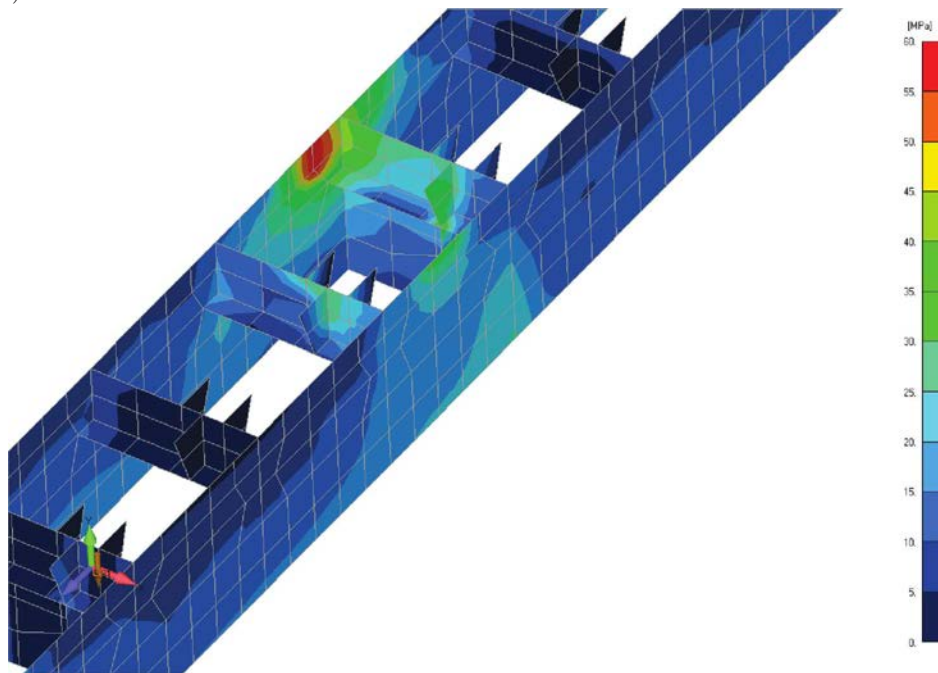


FIG. 10. FEM Analysis – distribution of the reduced stresses in the under rail beam:
a) original, b) with additional ribs.

Table 1. Selected FEM results for bridge beam elements (in brackets with ribs).

Under rail beam part	Reduced Stresses [MPa]		
	load variant:		Fatigue category acc. to [4]
	1 – carriage on the short leg	2 – carriage in the middle of span	
Side shells	60 (59)	53 (52)	160
Membrane	65 (65)	65 (64)	100
Weld “B” & “Z” type	65 (44)	57 (41)	57

() – stress level with additional ribs.

Also examined the stress for sticking strain gauges of T1, T2 and rosettes R1, R2 and R3. Table 2 gives the highest stress values obtained for the analyzed positions of the carriage, which is in good agreement with values obtained with the strain gauge measurements. It is worth noting that these values also take into account the load from the weight of his own design.

Table 2. Stress values for T1, T2 and R1, R2, R3 places.

Measurement place	Recorded maximum stress at load of	
	self weight	self and carriage weight
T1	$\sigma_1 = 10$ MPa	$\sigma_1 = 33$ MPa
T2	$\sigma_1 = 13$ MPa	$\sigma_1 = 38$ MPa
R1	$\sigma_z = 12$ MPa	$\sigma_z = 18$ MPa
R2	$\sigma_z = 6$ MPa	$\sigma_z = 32$ MPa
R3	$\sigma_z = 8$ MPa	$\sigma_z = 18$ MPa

4. THE RESULTS OF NUMERICAL ANALYSIS OF THE STRESS STATE WITH REGARD TO THE MEASUREMENTS ON THE OBJECT REAL

The bases no the FEM stress analysis, was selected areas crane structure in which the strain gauge measurements were performed [7]. The first area is in the middle of the span length in the area under rail beam and a second on the shell bridge behind long support leg.

4.1. Measurement procedure

For the measurements used three rosette strain gauges tagged R1, R2, R3 type **TFxy-4/120** and two single strain gauges T1 and T2. Each strain gauge is

temperature-compensated by a compensating gauge, identical as the one used for measurements.

The whole measurements included four measurement cycles. The first three cycles covered when driving the carriage at the stop bridge. The fourth cycle included ride of the entire bridge at carriage parked on the support short.

Cycle I – ride carriage “on empty” from support short to long support leg.

Cycle II – ride from short to long support (in the area of the long support loading of iron ore)

- ride to support short with ore,
- back to long support and dropping loads,
- stop to support long.

Cycle III – carriage parked on the support long (loading of iron ore)

- ride to support short with ore
- back to long support and dropping loads,
- ride carriage “on empty” to support short.

Cycle IV – ride of the entire bridge at carriage parked on the support short.

Arrangement diagram strain gauges rosettes R2, R3, T1, T2 in the middle of the span length in the area under rail beam between the ribs Number 14 and 15 on the western side of the bridge, and on the shell on the western side of the bridge behind long support leg mounted strain gauges rosette R1, shown in Fig. 11. Figure 12 shows mounted on the shell of the bridge rosette R1 and single strain gauges in the area under rail beam T1 (mounted on the shell) and T2 (mounted on C300 profile)

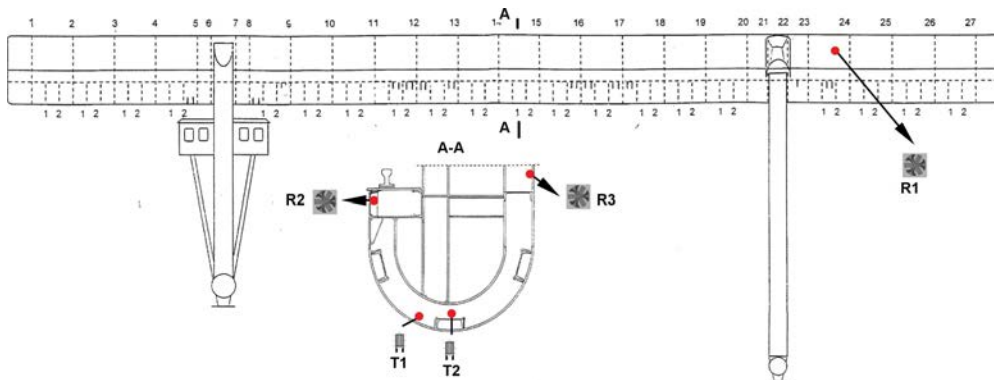


FIG. 11. Arrangement diagram strain gauges.



FIG. 12. Rosette R1 and single strain gauges T1 and T2 mounted crane structure.

4.2. Measuring equipment

Measurements are taken with an amplifier HMB MGCplus utilising resistance or induction sensors. The bridge is supplied from gel batteries 12V-12Ah and the entire circuit is connected to a portable computer (laptop) supported by the professional programme “Catman” (HMB) to record the measurement data. The measurement equipment is shown in Fig. 13.



FIG. 13. Measuring equipment.

4.3. Development of measurement results

The maximum measured stress values were recorded during the second measurement cycle on C300 profile in the lower part of the rail beam where the strain gauge mounted T2 and on the bottom of the shell where the strain gauge mounted T1.

For rosettes R2 and R3 increase in stress values observed during the approaching carriage to plane mounted rosettes where the greatest stress occurred during invasion of carriage in the place of sticking the rosette and when the carriage moves away stress decreased.

The greatest stress were registered by the rosette R2 (Fig. 15) located under the rail beam and amounted to about 31 MPa and the rosette R3 stress on the shell of the bridge were about 10 MPa.

For rosette R1 mounted on the shell on behind long support leg to observe it is possible increase in stresses when approaching the carriage to long support leg where the value of the maximum stress of about 10 Mpa.

It should be noted that the carriage ride always ended in the axis long support leg not entering on the overhang behind support where it was mounted rosette R1.

Figure 14 show graphs of stress for the second cycle registered by the single strain gauges T1 and T2 and in Fig. 15 show graphs of reduced stresses for the second cycle registered by the strain gauges rosettes R2, R3, R3.

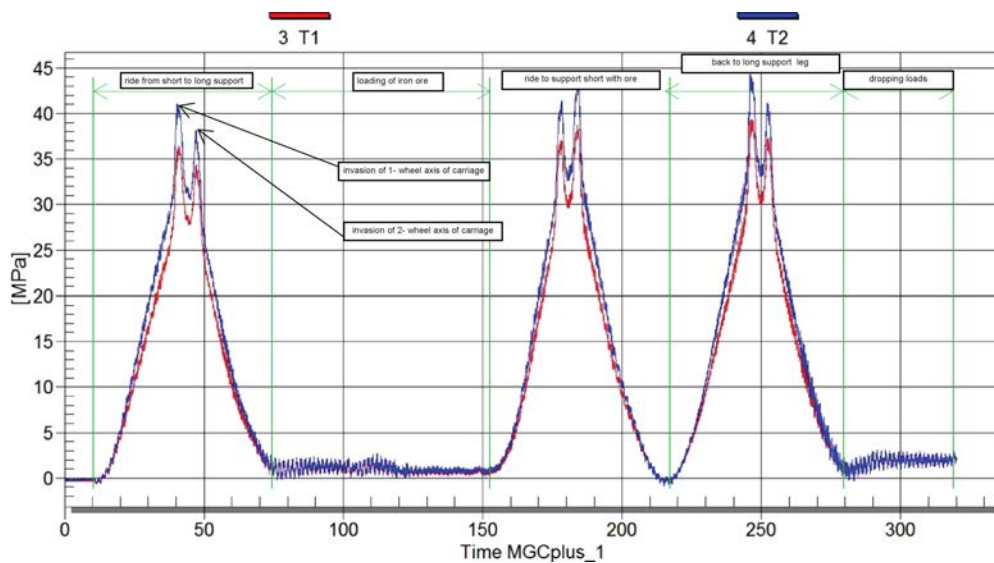


FIG. 14. Figure stress σ_1 at the time of the second cycle registered by the T1 and T2.

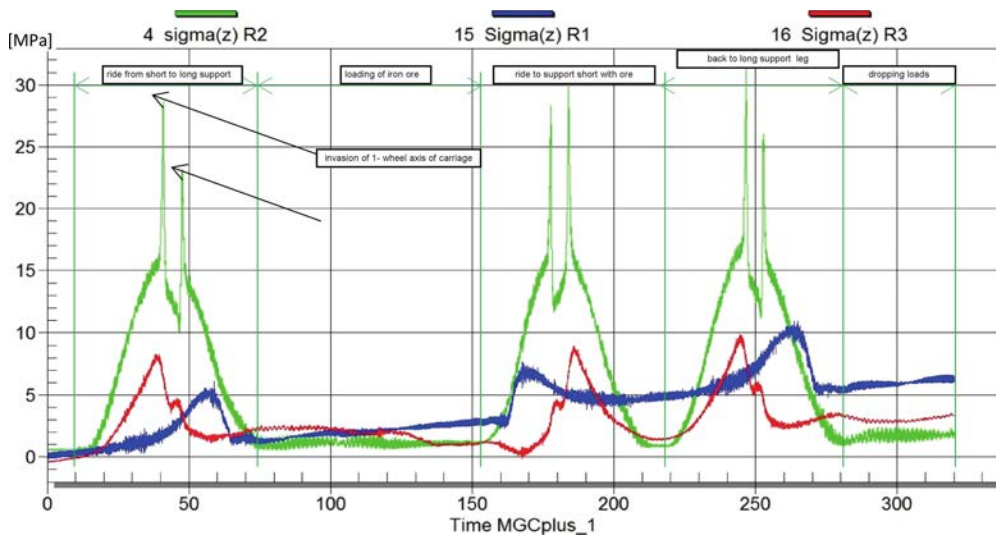


FIG. 15. Figure reduced stresses σ_z during the second cycle registered by the R1, R2 and R3.

While driving bridge – the fourth cycle, the strain gauges T1, T2 observe double-sided asymmetrical cycles a small amplitude change of stress of about 1.5 MPa shown in Fig. 16. and the values of reduced stress for R1, R2, R3 are a maximum of 4 MPa shown in Fig. 17.

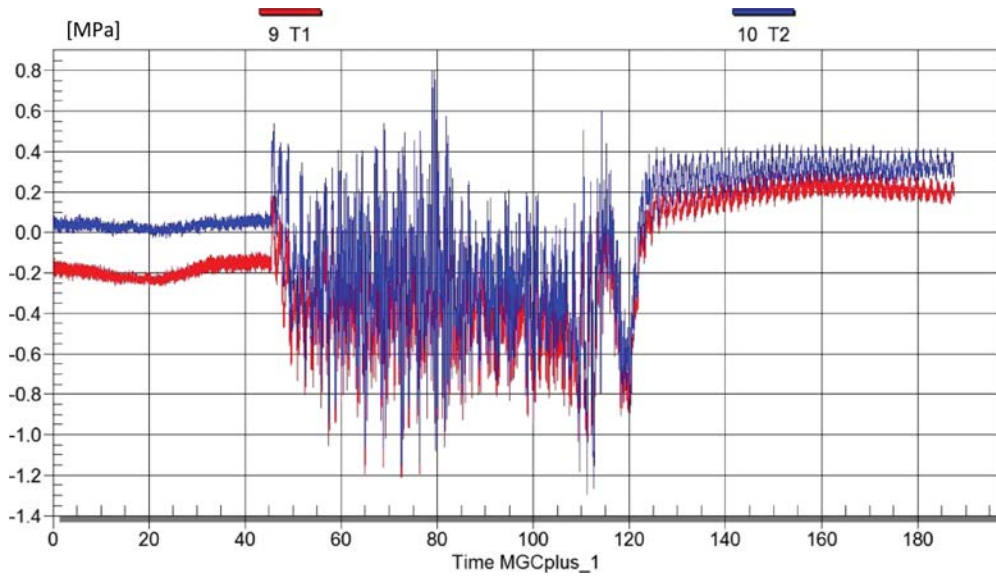


FIG. 16. Figure stress σ_1 at the time of the fourth cycle registered by the T1 and T2.

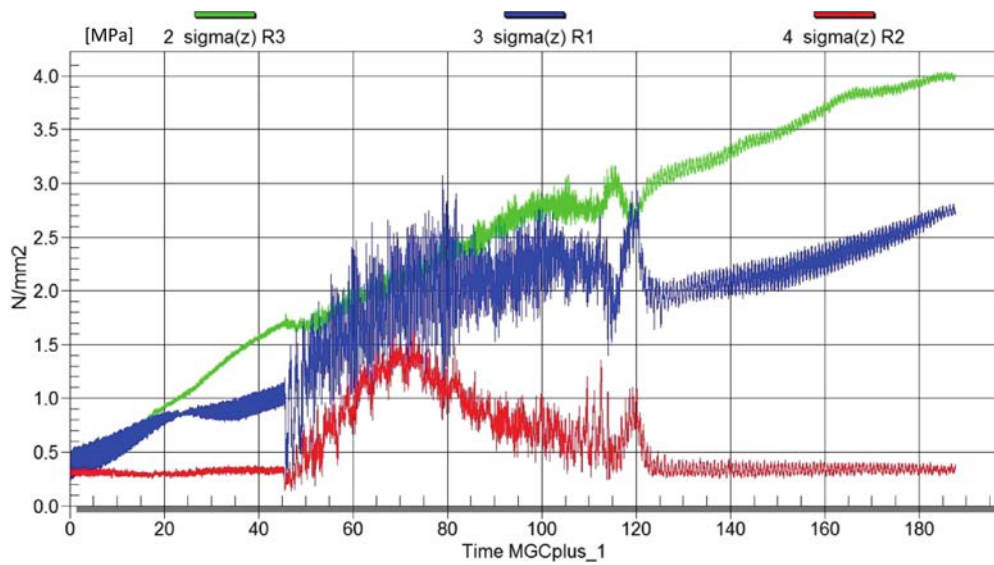


FIG. 17. Figure reduced stresses σ_z during the fourth cycle registered by the R1, R2 and R3.

Table 3 lists the most reduced σ_z [MPa] by stress HMH hypothesis for rosettes R1, R2, R3 and axial stresses σ_1 [MPa] for strain gauges T1, T2 which appeared for individual measuring cycles.

Table 3. Results achieved of conducted examinations.

Strain gauge	Cycle I σ_z [MPa]	Cycle II σ_z [MPa]	Cycle III σ_z [MPa]	Cycle IV σ_z [MPa]
R1	6	10	10	2.5
R2	24	31	31	1.5
R3	5	10	10	4
	Cycle I σ_1 [MPa]	Cycle II σ_1 [MPa]	Cycle III σ_1 [MPa]	Cycle IV σ_1 [MPa]
T1	31	39	39	1
T2	35	45	44	2

The measurements of strain gauges indicate the most strenuous areas of construction rail beams. Places of stress concentration of the correspond with the results obtained in the analysis of the FEM. Differences stress values obtained at the points sticking strain gauges and computer simulations to be a maximum of about 10% what allows to state the correctness of conducted examinations and made FEM stress analysis and read the maximum stress values considered reliable.

5. CONCLUSIONS

Made of gantry crane non-destructive testing showed the presence of numerous fatigue cracks, mainly in the area of the under rail beams whose origination sources have not been eliminated as a result of performing emergency repairs.

Based on analysis of FEM and strain gauge measurements on the real object, set the most strenuous areas of crane structures which correspond to the occurrence of fatigue cracks. Small differences not exceeding 15% in the values of stress obtained from strain gauge measurements and FEM computer simulations indicate correctness of the measurements of deformation and performed FEM stress analysis, and the obtained values of maximum stress can be regarded as a reliable.

Extreme reduced stress values for under rail beams before making reinforcements amounting to 65 MPa was obtained for the fillet welds type “B” and “Z” cracks area. As the source of “O” type cracks is often detected their neighborhood with cracks “B” and “Z”. The use of additional reinforcing ribs locally resulted in a reduction of stress in the area “B” and “Z” cracks of approx. 30%.

For the considered objects their life history is not known, but considering the fatigue category defined as 57 MPa [4] for the area where the cracks occurred, as the cause of the formation and development of fatigue cracks in the under rail beams can point that stress value exceeds the fatigue strength of considered welded joints. Reinforcements made in the under rail beams, had a significant impact on the reduction of the severity of fatigue cracks appearing.

The calculations and measurements can be used to execute a more thorough analysis of the fatigue life of the most intensive areas of crane construction.

REFERENCES

1. ŁADECKI B. *et al.*, *Gantry crane expertise in Zakład Wielkie Piece* [in Polish: *Ekspertyzy mostu przeladunkowego w Zakładzie Wielkie Piece*], PREH Sp. z o.o., Kraków 2003, 2010 and 2013.
2. ŁADECKI B., BOROWIEC W., *Geodetic monitoring as a nondestructive method in assessment of the technical state of constructions* [in Polish: *Monitoring geodezyjny jako nieniszcząca metoda oceny stanu technicznego konstrukcji*], Materiały 39 Krajowej Konferencji Badań Nieniszczących, Szczyrk 2010.
3. ŁADECKI B., BADURA S., MATACHOWSKI F., *Strength analysis of a gantry crane of coating structure*, *Mechanics and Control*, **31**, 3, 102–107, 2012.
4. PN-90/B-03200 *Steel structures. Design rules* [in Polish: *Konstrukcje stalowe. Obliczenia i projektowanie*].
5. ŁADECKI B., BADURA S., *Dynamic analysis of charging bridge of a shell structure*, *Journal of Civil Engineering, Environment and Architecture*, Oficyna Wydawnicza Politechniki Rzeszowskiej, Rzeszów 2014.

6. ZIENKIEWICZ O.C., TAYLOR R.L., *Finite Element Method* (5th Edition), Elsevier, 2000.
7. HOFFMANN K., *An Introduction to Measurements using Strain Gages*, Hottinger Baldwin Messtechnik GmbH, 1987.
8. FLUGGE W., *Stresses in Shells*, Springer-Verlag, 1973.
9. CARTZ L., *Nondestructive Testing*, ASM International, ISBN 978-0-87170-517-4, 1995.
10. HENRY F.D.C., *The design and construction of engineering foundations*, Chapman and Hall Ltd 1986.

Received October 27, 2014; revised version December 15, 2014.
